Short communication

Mg-doped $LiNi_{0.5}Mn_{1.5}O_4$ spinel for cathode materials

C. Locati [a,*], U. Lafont [a], L. Simonin [a], F. Ooms [b], E.M. Kelder [a]

[a] *TU Delft DelfChemTech Julianalaan 136, 2628 BL Delft, The Netherlands*
[b] *Solidion Research, Talmastraat 33, 2021 CL Haarlem, The Netherlands*

Abstract

Lithium-ion batteries are becoming more and more important not only for portable electronic devices, but also in prevision of high power electric vehicles. In such an optic, deep studies regarding all the components of a secondary battery are in development. In this study, high voltage cathode materials have been selected. Crystals with spinel structure have a 3D vacancy pathway suitable for Li-ions transport. The material under study was $LiNi_{0.5}Mn_{1.5}O_4$ doped with magnesium replacing the nickel. Various samples were synthesized via three different routes: a solid-state method, a modified sol–gel method and a xerogel method. The structure and morphology of the powders were analyzed with HRTEM and XRD. Electrochemical tests were also performed. A wide range of particle sizes (from micro to nanosize) was the result of the different synthesis routes. Unfortunately pure materials were not always obtained. The electrochemical tests showed improvement of the material's cyclability, by reducing the particle size. The electrochemical tests further confirmed the existence of a $Li_{1+d}Mn_{2-d}O_4$ impurity. The results are quite promising, however, further improvement of the purity of the electrode composition are needed.
© 2007 Elsevier B.V. All rights reserved.

Keywords: Lithium-ion battery; High voltage; Spinel; Cathode material

1. Introduction

Nowadays Li-ion batteries are the most promising rechargeable batteries, not only for electronic devices, but also in prevision of electric vehicles. Despite their high storage capacities, the power performance is still a crucial issue for implementing them in power tools. In order to increase the power, it is suggested to use nanomaterials. Nanostructures have a high surface/weight ratio that enhances the charge transfer. In addition, the diffusion/migration-length ratio is low, so the power performance can grow. These features are reflected in higher charge–discharge rates. The 3D vacancy pathway (suitable for Li-ion transport) was the main reason to choose spinel materials. Besides looking at the kinetics, we have chosen to study cathode materials providing high voltages, and, thus, a higher storage capacity can be expected. The system under study is $LiMg_{\delta}Ni_{0.5-\delta}Mn_{1.5}O_4$ with $\delta = 0.07$. Its theoretical capacity (C_{th}) is $148.7\,mAh\,g^{-1}$, very close to that of $LiMn_2O_4$ ($148.2\,mAh\,g^{-1}$).

The materials were synthesized via three different routes: a solid-state method (SS) [1], a modified sol–gel method (SG) [2] and a xerogel method (XG). Crystal structure, texture and morphology were analyzed via HRTEM, and XRD, while electrochemical tests were performed in CR2320 coin cells.

2. Experimental

2.1. Synthesis

The first procedure we adopted was a classical SS route. The precursors $LiOH \cdot H_2O$ (Fluka), $Mg(AC)_2 \cdot 4H_2O$ (Fluka), $Ni(AC)_2 \cdot 4H_2O$ (Aldrich) and $Mn(AC)_2 \cdot 4H_2O$ (Fluka) ($AC = CH_3COO$), were mixed with a blender au bain-marie at $80\,°C$ until the $Mn(AC)_2 \cdot 4H_2O$ was completely dissolved in its crystal water. The green solution obtained was put in an oven and fired. The calcination was done according to the following procedure to obtain best results: $10\,°C\,min^{-1}$ until $500\,°C$ and rest for 5 h, then $10\,°C\,min^{-1}$ until $100\,°C$ and rest for 12 h; $10\,°C\,min^{-1}$ until $800\,°C$ and rest for 12 h, then $1\,°C\,min^{-1}$ until $100\,°C$ and rest for 12 h. This procedure was repeated once again, then $10\,°C\,min^{-1}$ until $800\,°C$ and rest for 6 h, $0.1\,°C\,min^{-1}$ until $100\,°C$ and rest for 12 h. After every firing procedure, the powders were initially ground in a mortar before putting them in a

* Corresponding author. Tel.: +31 15 27 85536.
  E-mail addresses: c.locati@tudelft.nl
(C. Locati), info@solidion-research.com (F. Ooms).

planetary ball-mill with agate jars and balls (Fritsch Pulverisette 7). Milling was done at maximum speed for 30 min.

The second synthesis route was a SG method. The non-ionic triblock co-polymer Plurionic P123 surfactant (Aldrich), plus deionised water, was stirred thoroughly until it was complete mixed. The chelating molecule ethylene-glycol-butyl-ether ($\geq$99.5%, Aldrich) was added to slow down condensation. The same precursors of the solid-state synthesis were added to this solution. The solution was heated to 80 °C, kept at that temperature for 1 h au bain-marie, and then stirred for 24 h at room temperature before starting the calcination. Four steps were programmed without ball-milling in between, i.e., 1 °C min^{-1} until 180 °C and rest for 3 h; 10 °C min^{-1} until 500 °C and rest for 5 h; 10 °C min^{-1} until 800 °C and rest for 6 h and 0.1 °C min^{-1} until 300 °C and rest for 12 h. Finally the powders were ground in a mortar.

The third route was a classical acid-catalyzed sol–gel (XG). The same precursors of the solid-state method plus EtOH anhydrous (J.T. Baker) were stirred au bain-marie at 60 °C for 2 h. After stirring, a solution of urea/EtOH/H_2O (1:5:1 M) and 1 ml of HCl 0.3 M was added and stirred for 10 min. The solution was put in a crystallizer at room temperature for 1 week and in a dry-oven at 80 °C for another week. The substance obtained was ground in a mortar and put in an oven for two thermal treatments: the first one was 10 °C min^{-1} until 500 °C and rest for 5 h, while the second one was 10 °C min^{-1} until 800 °C and rest for 6 h, then 0.1 °C min^{-1} until 100 °C and rest for 12 h.

After the synthesis, the powders were tested electrochemically. The synthesized active materials were mixed with polyvinylidene fluoride (Solvay), carbon black (99.9+%, <1.0 µm; Alfa) and graphite ($\leq$0.1 mm; Fluka) with the following percentages 80:10:3:7, respectively and dissolved in 1-methyl-2-pyrrolydon (NMP, Merck-Schuschardt). The solution was ball-milled for 15 min and the pastes obtained were deposited on an aluminium strip with a 200 µm thick doctor blade and immediately dried at 80 °C for a couple of hours. The obtained electrode was pressed until it reached a mean thickness of 70 µm, samples of Ø14 mm were punched. The electrochemical tests were done in CR2320 type coin-cells (Hohsen), assembled in this order: can, electrode, Ø21 mm × 25 µm separator; PP gasket, four drops of electrolyte (1 M LiPF$_6$, EC/EMC/DMC 1:2:2 M Mitsubishi Chemical). Ø16 mm Lithium disk, Ø17 mm and 0.33 mm thick stainless steel spacer plate, Ø15 mm 1 t pre-pressed wave spring and cap with insulating adhesive tape on top to prevent short circuits during the manipulation. The coin-cells were sealed in a He-filled glove-box (H_2O < 5 ppm). During the charge–discharge tests, the coin cells were kept under pressure with Hoffman clamps to ensure good electrical contacts.

2.2. Characterization techniques

The structure of the powders was investigated with an X-ray diffractometer (XRD, Bruker AXS D8 advance, Cu Kα). Every diffraction pattern was taken without Kα_2 stripping. The size of the crystals was estimated by applying the Scherrer formula [3].

The crystallinity was studied with a transmission electron microscope (TEM) Philips CM30T with a LaB$_6$ filament as the source of electrons at 300 kV. Samples were mounted on Quantifoil$^©$ microgrid carbon polymer supported on a copper grid by placing ground sample on the grid.

The battery tests were performed with a Maccor S4000 tester at room temperature using different procedures to charge and discharge the batteries. Li-ion batteries were tested to study the voltage profile, the cycling behaviour and the rate capability of the synthesized cathode material. The tests were done by galvanostatic cycling in a potential range between 3.5 and 4.9 V. Various rates were used to verify the rate capability. Thereto five cycles were run for each current. *C*-Rates have been chosen between 0.1*C* and 5*C*, reflecting charge and discharge of the full capacity of Li$_x$Mg$_{007}$Ni$_{0.43}$Mn$_{1.5}$O$_{4-x}$ being 1, i.e., which is 148.7 mAh g^{-1}.

3. Results and discussion

At the end of the first firing step, powders from the sol–gel and xerogel method were dark grey with some orange and/or green impurities. That indicates the possible presence of Li$_{1+d}$Mn$_{2-d}$O$_4$ and Li$_x$Ni$_{1-x}$O, respectively. The powders made via the SS route were only dark grey. The ball-milling procedure after the first oven rate allowed the impurities to mix with the main compound and, hence, to react forming pure materials in the following annealing step.

3.1. XRD analysis

All the XRD patterns in Fig. 1 showed spinel structures. The impurities are not observed in the patterns: LiMn$_2$O$_4$ is a spinel, and has almost the same peak position as the material under study. Similarly Li$_2$MnO$_3$, having the rock salt structure, has peak position almost at the same place of LiMn$_2$O$_4$. However, the peaks of Li$_x$Ni$_{1-x}$O, an impurity that was reported by others, could not be observed above the noise [1]. Finally the XRD results showed that the powders made via the SS have the sharpest peaks.

Table 1 lists the grain sizes calculated by the Scherrer equation and the particle sizes estimated by TEM pictures (Fig. 2). It
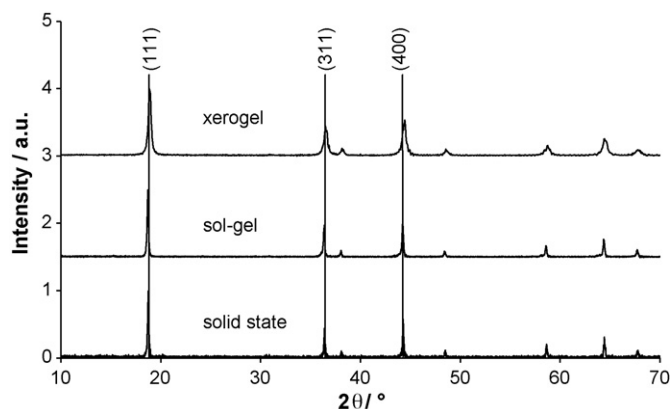

Fig. 1. XRD patterns of the spinel samples divided by synthesis route.

Table 1
Grain sizes calculated by the Scherrer equation and particle size estimated by the analysis of TEM pictures

Synthesis method	Scherrer, grain size (nm)	TEM analysis, particle size (nm)
SS	70–250	50–300
SG	80–200	50–200
XG	40–150	10–200
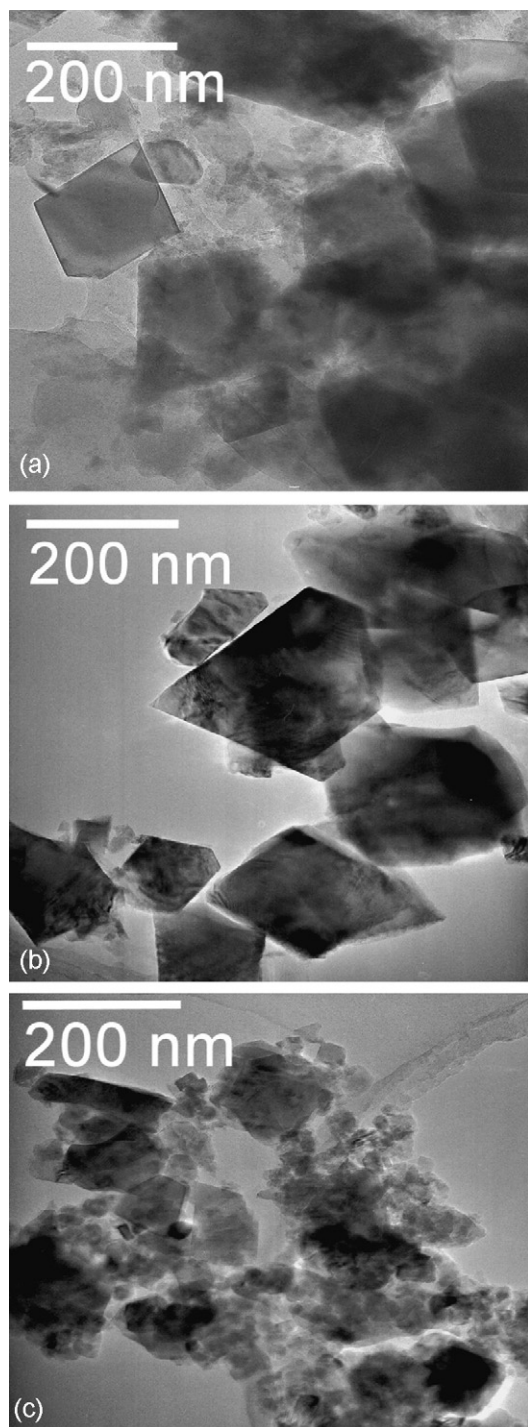
should be noted that a particle is defined as a unit of an agglomerate. A particle may contain one or more grains (domains). These grains are the basic diffraction units responsible for the XRD peak broadening. The SS route leads to the biggest grains, while smaller dimensions can be reached with the SG method. The smallest particles are obtained with the XG method, but always together with bigger grains. In both cases, these crystals are highly agglomerated. Nevertheless, the sizes measured with XRD seem to be concordant with the sizes obtained with TEM.

3.2. Morphological analysis

Fig. 2 shows TEM pictures of the samples. The SS route results in crystals of the order of 200 nm (Fig. 2a), while in the SG powders also small crystals are present (Fig. 2b). In contrast, particles realized with the XG routes (Fig. 2c) are in the order of 50 nm and less.

It is believed however that a different choice of precursors and optimization of the synthesis parameters (temperature, dwell time, etc.) may improve the purity of the samples and could bring a narrower particle size distribution [4].

3.3. Electrochemical tests

Charge–discharge tests were performed in CR2320 coin cells. A 0.1C C-rate was used for all the charge procedures, and we adopted different C-rates for the discharge procedures: 0.1C, 0.2C, 0.5C, 1C, 2C and 5C for five cycles each, and then back to 0.2C in the end. With this procedure it is not only possible to see the intercalation behaviour of the cathode during different discharge rates, but it is also possible to understand if the battery can recover the capacity after a long stress period.

To understand the electrochemical behaviour, Fig. 3 shows the voltage versus capacity plot at 0.2C (first discharge curve) for the investigated materials. In all the cases, the voltage plateau around 4.7–4.8 V is present, reflecting the Ni oxidation. The other plateau at 3.9–4.1 V can be related to the presence of side products $Li_{1+d}Mn_{2-d}O_4$ and/or Li_2MnO_3 and, hence, the plateau reflects the Mn oxidation [5]. These impurities, anyway,

Fig. 2. TEM pictures of powders made with solid-state (a), sol–gel (b) and xerogel route (c).
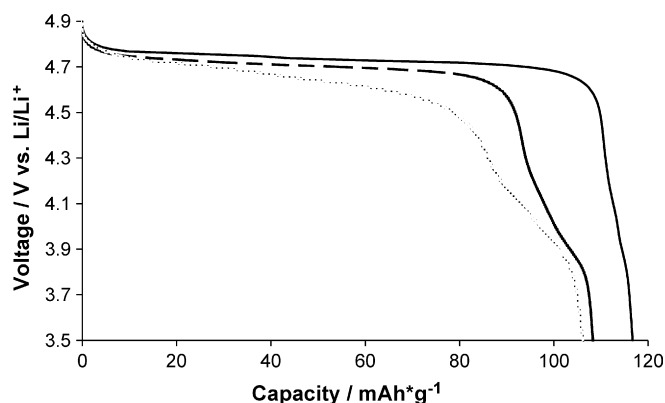

Fig. 3. Voltage vs. capacity plot of the discharge of the first cycle at 0.2C. SS: solid line, SG: dashed line, XG: grey line.

contribute for 4% of the overall capacity in the solid-state sample, for 13% in the sol–gel sample and for 19% in the xerogel sample. Although suggested initially, Mn is an impurity phase; it may also be part of a solid solution as XRD did not showed these impurities.

The capacities of the powders synthesized by the various methods and measured at a 0.2 C-rate are very close to each other, i.e., 116 mAh g^{-1} for the SS, 108 mAh g^{-1} and 106 mAh g^{-1} for the SG and XG, respectively (see Fig. 3).

In order to verify the rate capability of the various samples, capacities have been normalized to 100% capacity for the fifth value measured at a 0.2 C-rate. The results are plotted per sample showing the different rate performances (Fig. 4a–c). In Fig. 5 these results are gathered in one picture for comparison.

From the above figures, it is clear that LiMg$_{0.07}$Ni$_{0.43}$Mn$_{1.5}$O$_4$ made with the SS method (Fig. 4a), has the high-
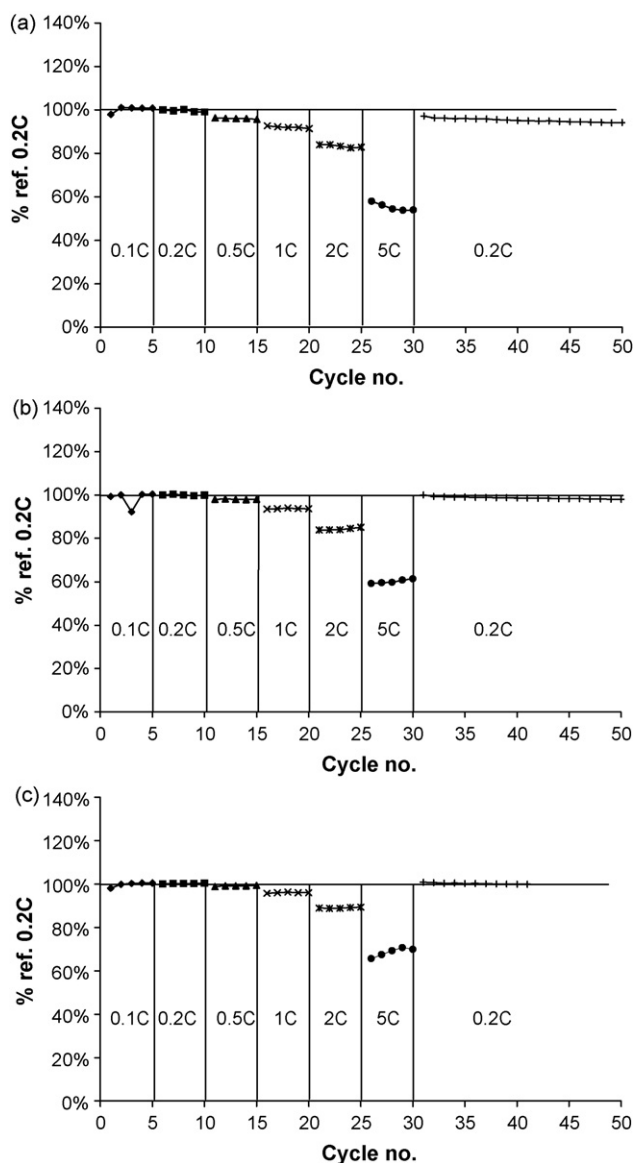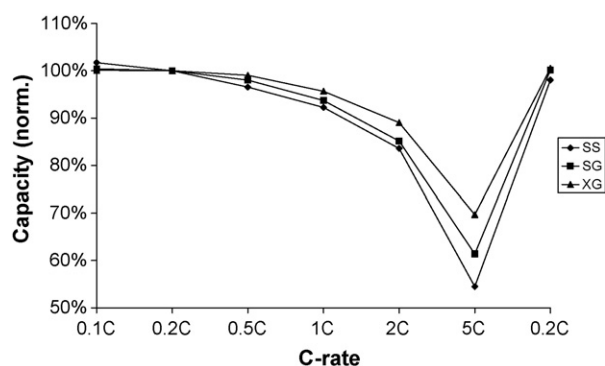

Fig. 5. Fifth discharge capacity of each C-rate.

est capacity loss at high C-rates. Besides, the battery does not recover the initial capacity at 0.2C. In that respect, the sol–gel samples showed better results, i.e. the capacity retained and good stability was achieved (Fig. 4b). For the xerogel sample the results seem to be even better. Also at 1C the loss of capacity is small, and at 5C the capacity still reaches 70% of the nominal capacity (0.2C). Besides, the capacity recovery at 0.2C is complete (Fig. 4c).

4. Conclusions

In order to synthesize high voltage cathode materials, this research was focused on the fabrication of nanopowders of LiNi$_{0.5}$Mn$_{1.5}$O$_4$ doped magnesium. The synthesis routes lead to spinel phases that may have impurities (spinels or other cubic phases) or solid solutions in which it is not clear whether there is cluster formation.

The SS method gave a narrow size distribution but particles in the sub-micron range. On the other side, the SG and XG routes also gave sub-micron particles of single crystals, but together with nanoparticles. All the techniques allow us to synthesize single crystals from 10 to 300 nm (Table 1 and Fig. 2a–c).

Battery tests showed good cyclability for the material made with different synthesis routes. The best performances of capacity, rate capability and stability were obtained with the SG synthesis, in particular at high C-rates. The XG route, seen as a variant of the sol–gel, gave similar electrochemical results.

Future work will focus on controlling the composition and the synthesis methods for obtaining even smaller particles, i.e. below 20 nm, with a narrower size distribution. Besides, optimization of the electrode composition will be another important test.

Acknowledgements

Fig. 4. Discharge plots vs. number of cycles divided by synthesis route: (a) solid-state; (b) sol–gel; (c) xerogel.

References

[1] F.G.B. Ooms, E.M. Kelder, J. Schoonmann, M. Wagermaker, F.M. Mulder, Solid State Ionics 152–153 (2002) 143–153.

[2] U. Lafont, P. Kooyman, A. Galarneau, F. di Renzo, Stud. Surf. Sci. Catal. 155 (2005) 355–366.

[3] A.L. Patterson, Phys. Rev. 56 (10) (1939) 978–982.

[4] U. Lafont, C. Locati, E.M. Kelder, Solid State Ionics 177 (2005) 3023–3029 (Sp. Iss. SI November 30, 2006).

[5] D. Guyomard, J. Tarascon, Solid State Ionics 69 (1994) 222.